THE ASTROPHYSICAL JOURNAL, 378:6–16, 1991 September 1

CONFIRMATION OF DUST IN DAMPED LYMAN-ALPHA SYSTEMS

YICHUAN C. PEI[1] AND S. MICHAEL FALL
Space Telescope Science Institute, 3700 San Martin Drive, Baltimore, MD 21218
AND
JILL BECHTOLD
Steward Observatory, University of Arizona, Tucson, AZ 85721
Received 1990 November 13; accepted 1991 March 4

ABSTRACT

As part of a search for dust at high redshifts, we have acquired new spectra of quasars in the Wolfe et al. sample: 13 with damped Lyα systems along the lines of sight and 15 without. Our spectra cover the region 3950–6900 Å at a resolution of 15 Å with signal-to-noise ratios of 10–50. We have determined spectral indices over a common range of wavelengths in the rest frames of the quasars between Lyα and C IV emission. Several internal and external checks indicate that the typical errors in the spectral indices are ± 0.1. We find that quasars with damped Lyα systems in the foreground are stochastically redder than those without damped Lyα systems in the foreground. This difference, significant at the 3 σ level, confirms our previous detection in the sample of Sargent, Steidel, & Boksenberg. Combining the Wolfe et al. and Sargent et al. samples increases the significance of the reddening to at least 4 σ. We compute dust-to-gas ratios from the spectral indices on the assumption that the extinction curve in the damped Lyα systems has the same shape as that in the Milky Way or the Large or Small Magellanic Cloud. Galactic-type dust appears to be ruled out by the absence of strong extinction near 2175 Å in the rest frames of several damped Lyα systems. Our best estimates of the typical dust-to-gas ratio in the damped Lyα systems are then 5%–20% of that in the Milky Way. This result, together with recent measurements of the gas-phase abundances of Zn and Cr in three damped Lyα systems, indicates that the overall abundances of heavy elements (in both the gas and solid phases) are about one order of magnitude lower than the Galactic value.

Subject headings: cosmology — galaxies: intergalactic medium — quasars

1. INTRODUCTION

This is the third in a series of papers on the reddening and obscuration of quasars by dust in damped Lyα absorption systems (Fall & Pei 1989, hereafter Paper I; Fall, Pei, & McMahon 1989, hereafter Paper II). The damped Lyα systems contain most of the neutral atomic hydrogen in the universe at redshifts $2 \lesssim z \lesssim 3$, very little molecular hydrogen, and some heavy elements (Wolfe 1988, 1990, and references therein). They are generally thought to be the high-redshift analogs or progenitors of ordinary galactic disks, but because their linear sizes are known in only one or two cases, it is also possible that they represent a highly inflated population of dwarf galaxies (Tyson 1988). The abundance of dust is relevant to studies of the chemical enrichment and the transfer of Lyα and continuum radiation in the damped Lyα systems. To search for reddening, we compare the spectral indices of quasars with and without damped Lyα systems along the lines of sight. From this, we deduce the typical extinction and dust-to-gas ratio in the damped Lyα systems. While our method is straightforward in principle, it requires in practice that the selection of quasars be unbiased with respect to absorption features and optical colors and that the errors in the spectral indices be smaller than the intrinsic dispersion among quasars.

We have previously searched for reddening in two large samples: that of Wolfe et al. (1986, hereafter WTSC) and that of Sargent, Steidel, & Boksenberg (1989, hereafter SSB). The quasars in both samples were chosen from existing catalogs on the basis of their emission redshifts and apparent magnitudes. Most of the quasars were originally discovered in objective-prism surveys, but some of them were found in radio and X-ray surveys; only one quasar in each of the samples was discovered on the basis of its optical colors. Thus, as regards the selection of quasars, both the WTSC and SSB samples are suitable for our analysis. There are, however, important differences in the accuracy of the spectral indices. From the WTSC sample, we could only set upper limits on reddening in the damped Lyα systems (Paper I), whereas, from the SSB sample, we were able to detect a small amount of reddening (Paper II). The WTSC survey was designed to search for damped Lyα systems, not to determine spectral indices. Consequently, there was no need to attempt accurate spectrophotometry or to cover the region redward of Lyα emission.

In this paper, we present spectra of quasars in the WTSC sample with sufficient accuracy and spectral coverage for a detection of reddening in the damped Lyα systems. The motivation for another search is that our detection in the SSB sample, at the 3 σ level, needs confirmation in an independent sample and over a wider range of H I column densities. By combining the WTSC and SSB samples, we can make an even stronger test for reddening in the damped Lyα systems. In § 2, we describe our observations and the determination of spectral indices. Our estimates of the dust-to-gas ratio in the damped Lyα systems are given in § 3 for the WTSC sample and in § 4 for the SSB and combined samples. In § 5, we derive upper limits on the abundance of Galactic-type dust in several damped Lyα systems, and in § 6, we discuss our results in terms of the chemical enrichment of the damped Lyα systems.

[1] Present address: Princeton University Observatory, Peyton Hall, Princeton, NJ 08544.

Throughout this paper, the subscripts *e*, *a*, and *o* refer, respectively, to emission, absorption, and observation.

2. OBSERVATIONS AND SPECTRAL INDICES

Our goal was to observe all 14 quasars in the WTSC sample with confirmed damped Lyα systems in the foreground (the "damped subsample") and an equal number of quasars in the WTSC sample without damped Lyα systems in the foreground (the "control subsample"). Monte Carlo simulations indicated that a larger control subsample would increase only slightly the sensitivity of our search for reddening. We observed the 28 quasars listed in Table 1—13 in the damped subsample and 15 in the control subsample. The observations were made in 1989 November and 1990 June with the Steward Observatory 90 inch telescope, Boller and Chivens spectrograph, and Texas Instruments CCD detector. We used a 300 line mm^{-1} grating blazed at 6900 Å in first order and a 4".5 slit to obtain spectral coverage of 3950–6900 Å at a resolution of 15 Å (FWHM). Second-order light was eliminated by an order-blocking filter. We observed each quasar for 1200–6600 s, with the longer integrations divided into two or three exposures, and the slit oriented at the average parallactic angle for each exposure. The atmosphere was rarely photometric, and the seeing was usually in the range 2"–4". We also observed several IIDS standard stars at the beginning, middle, and end of each night, through airmasses that bracketed those of the quasars. Bias frames were taken at the beginning of each night, and quartz-lamp flat fields and He-Ne-Ar arc exposures were taken after the observations of each quasar and standard star.

We reduced the observations by standard procedures using several IRAF packages. Figure 1 shows the resulting spectra and the 1 σ error arrays derived from photon statistics. The signal-to-noise ratios are typically 10–50 per pixel. We determined the spectral indices, defined by $f_\nu \propto \nu^{-\alpha_o}$, or equivalently $f_\lambda \propto \lambda^{\alpha_o - 2}$, between Lyα and C IV emission, i.e., over the common range $1216 \lesssim \lambda_e \lesssim 1549$ Å in the rest frames of the quasars. In these continuum fits, emission and absorption features exceeding a 3 σ threshold were removed iteratively until the remaining RMS positive and negative residuals were equal. The errors in α_o caused by photon statistics and other deviations from pure power laws are typically ± 0.07. We corrected the spectral indices of five quasars for Galactic reddening using the Burstein & Heiles (1982) maps; the other quasars have $E_{B-V} \lesssim 0.03$ and therefore $\Delta\alpha_o \lesssim 0.12$. We also computed

TABLE 1

OBSERVATIONS

Quasar	Discovery[a]	z_e[b]	Subsample[c]	UT Date	Exposure	α_o	m_{1450}
Q0049+014	O	2.31	C	1989 Nov 26	3000 s	0.99	17.4
Q0100+130	C	2.68	D	1989 Nov 27	3000	0.84	17.4
Q0109+022	O	2.35	C	1989 Nov 27	3000	0.36	17.7
Q0123+257	R	2.36	C	1989 Nov 26	1150	0.17[d]	18.5
				1989 Nov 27	1650		
				1989 Nov 28	3000		
Q0149+336	R	2.43	D	1989 Nov 28	3000	0.90	18.2
Q0207−003	O	2.84	C	1989 Nov 28	3000	0.54	17.6
Q0458−020	R, X	2.29	D	1989 Nov 27	3000	1.56[d]	19.1
				1989 Nov 27	3000		
Q0805+046	R, X	2.88	C	1989 Nov 4	3000	0.75	18.7
Q0819−032	R	2.35	C	1989 Nov 27	1800	0.33[d]	19.4
				1989 Nov 27	3000		
Q0820+296	R	2.37	C	1989 Nov 27	3000	0.42	19.2
Q0831+128	O	2.75	C	1989 Nov 4	2400	0.66	18.5
Q1136+122	O	2.89	D	1990 Jun 22	2400	1.00	18.6
Q1151+068	O	2.76	D	1990 Jun 24	3600	0.90	18.5
Q1215+333	R	2.60	D	1990 Jun 22	3000	0.32	18.5
Q1244+347	O	2.48	D	1990 Jun 24	3000	0.64	19.3
Q1318−113	O	2.31	C	1990 Jun 25	1200	1.09	18.0
Q1337+113	O	2.92	D	1990 Jun 24	3000	1.51	19.7
Q1347+112	O	2.70	D	1990 Jun 25	3600	0.96	19.2
Q1358+115	O	2.57	C	1990 Jun 23	1300	1.10	17.7
				1990 Jun 23	2000		
Q1402−012	R	2.52	C	1990 Jun 25	2500	0.57	18.6
Q1455+123	O	3.06	C	1990 Jun 22	3600	0.59	19.6
Q1623+268A	O	2.49	C	1990 Jun 24	1500	0.36	19.1
				1990 Jun 24	3000		
Q1623+268B	O	2.52	C	1990 Jun 22	3000	0.31	17.5
				1990 Jun 23	3000		
Q2136+141	R	2.43	D	1989 Nov 28	3000	2.91[d]	19.6
				1990 Jun 24	3600		
Q2206−199N	O	2.54	D	1989 Nov 28	3000	0.81	17.8
Q2256+017	R	2.66	C	1990 Jun 22	3600	0.58[d]	18.9
Q2348−011	O	3.01	D	1989 Nov 28	3000	0.89	19.2
Q2359−022	O	2.82	D	1989 Nov 28	3000	0.89	19.3

[a] Method of discovery from Hewitt & Burbidge 1987: objective prism (O), radio (R), X-ray (X), color/UV-excess (C).
[b] Emission redshift from Hewitt & Burbidge 1987.
[c] Subsample according to Turnshek et al. 1989: damped (D), control (C).
[d] Spectral index before correction for Galactic reddening: 0.45 (Q0123+257), 1.79 (Q0458−020), 0.63 (Q0819−032), 3.20 (Q2136+141), 0.78 (Q2256+017).

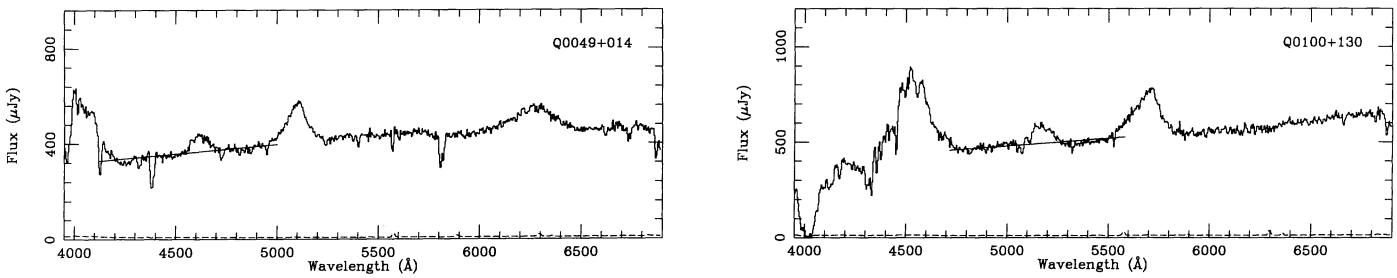

FIG. 1.—Spectra of quasars in the WTSC sample. The solid lines are the power-law fits between Lyα and C IV emission described in § 2. The dashed curves show the 1 σ error arrays.

apparent magnitudes m_{1450} from the continuum fluxes at the emission wavelength $\lambda_e = 1450$ Å. The values of α_o and m_{1450} are given for each quasar in the last two columns of Table 1. To estimate the overall uncertainties in our measurements, we have compared the results from different exposures of the same quasar and the same exposures calibrated with different standard stars. The inferred errors are typically ± 0.1 in α_o and ± 0.2 in m_{1450}. We have also compared our spectral indices and apparent magnitudes with those of SSB for the four quasars in common (Q0207−003, Q0805+046, Q2348−011, and Q2359−022). The mean differences (us minus SSB) are -0.08 ± 0.08 in α_o and $+0.22 \pm 0.14$ in m_{1450}.

Figure 2 shows histograms of the observed spectral indices in the damped and control subsamples. Evidently, the quasars with damped Lyα systems along the lines of sight are stochastically redder than those without damped Lyα systems along the

FIG. 1.—*Continued*

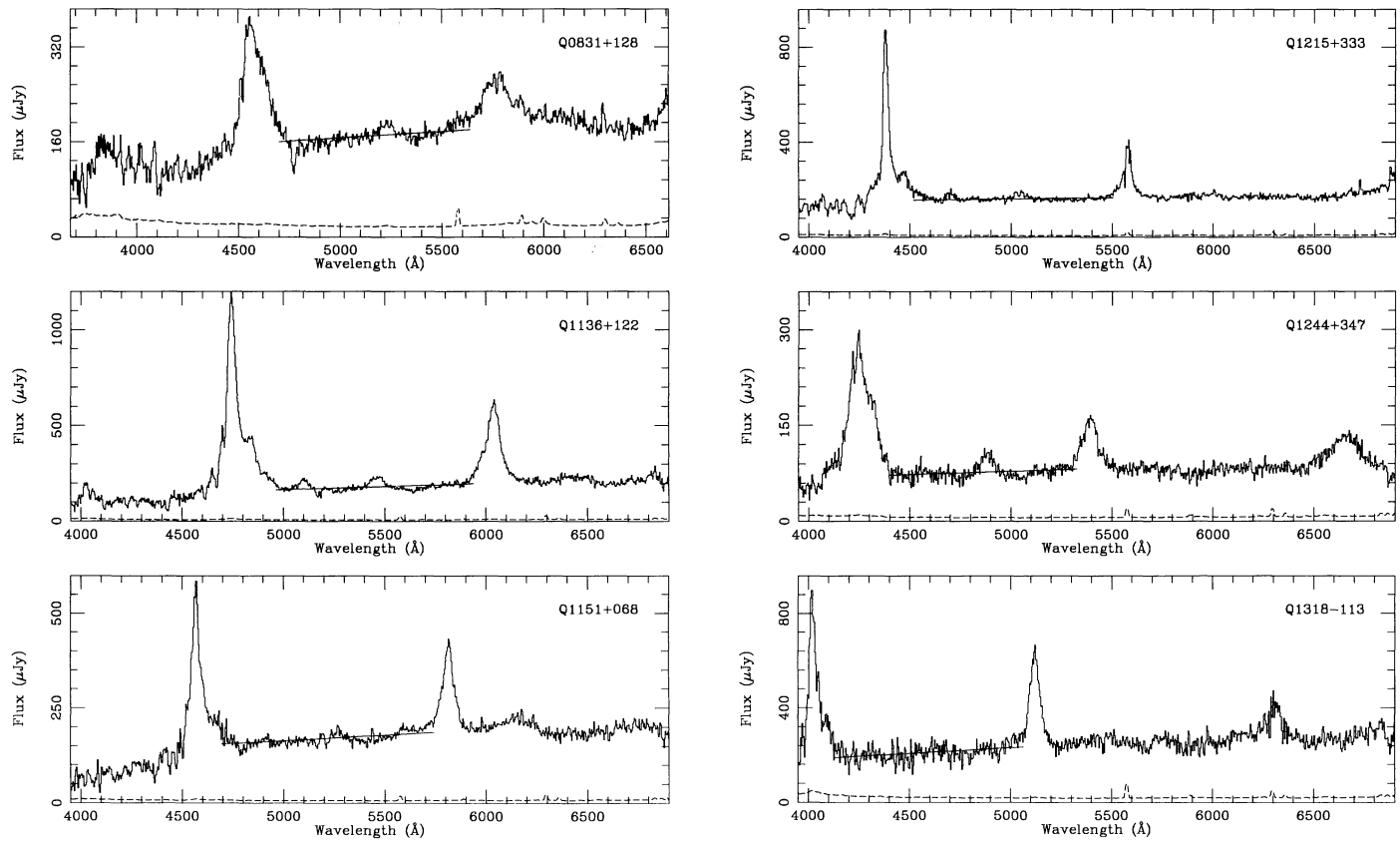

FIG. 1.—*Continued*

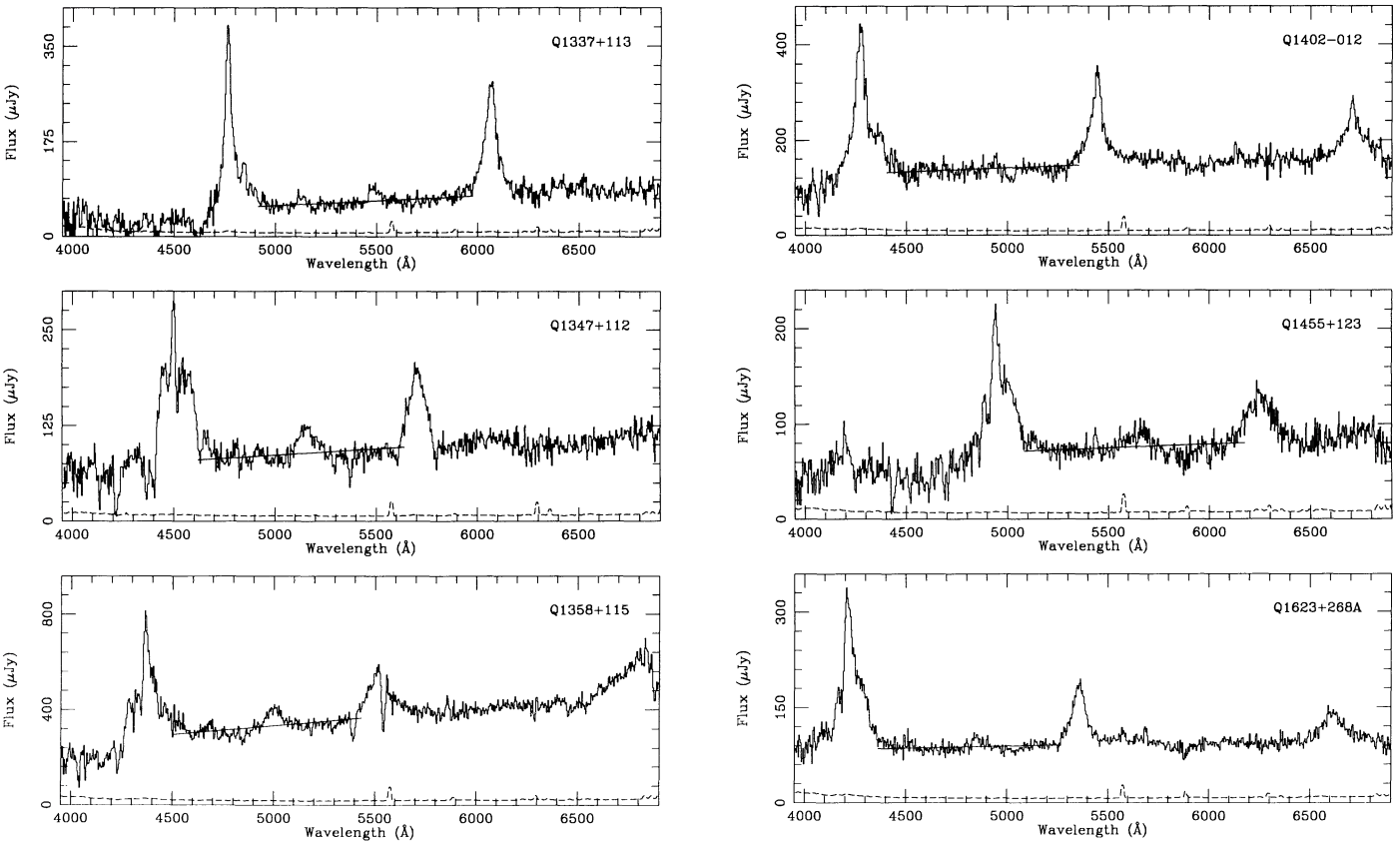

FIG. 1.—*Continued*

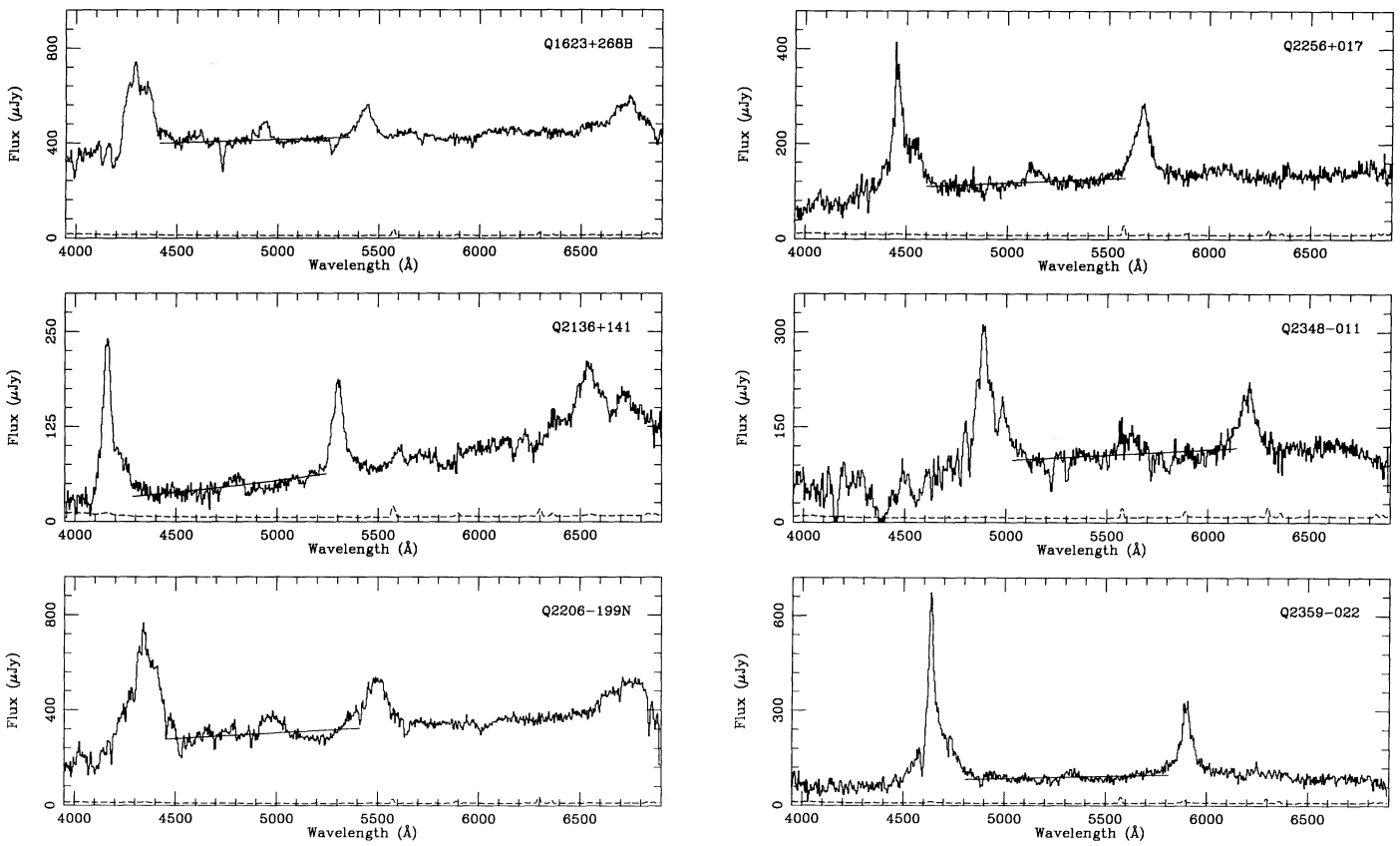

FIG. 1.—*Continued*

lines of sight. This difference is significant at the 99.6% level according to a Mann-Whitney U-test and confirms our previous detection of reddening. The mean spectral indices in the damped and control subsamples are, respectively, $\langle \alpha_o^d \rangle = 1.09 \pm 0.17$ and $\langle \alpha_o^c \rangle = 0.59 \pm 0.07$. We have checked that the distributions of emission redshifts z_e and apparent magnitudes m_{1450} in the two subsamples are statistically indistinguishable. There is some evidence from the SSB spectra that radio-loud quasars are redder on average than radio-quiet quasars, a trend that appears only weakly in our observations. However, the fraction of radio-loud quasars in the damped subsample (four out of 13) is slightly lower than the corresponding fraction in the control subsample (six out of 15). We can therefore assume that the observed reddening is caused by dust in the damped Lyα systems rather than radio sources in the background quasars.

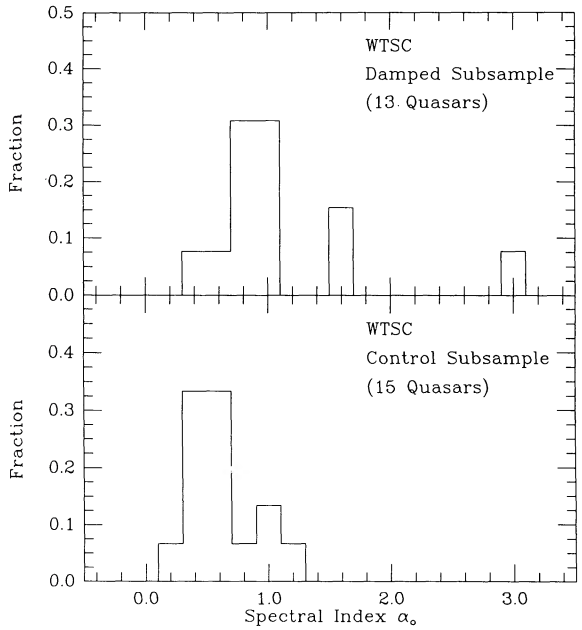

FIG. 2.—Histograms of the observed spectral indices in the WTSC damped and control subsamples. The former are redder than the latter at the 99.6% confidence level. The reddest quasar is Q2136+141.

3. DUST-TO-GAS RATIOS: THE WTSC SAMPLE

We now estimate the dimensionless "dust-to-gas ratio" $k \equiv 10^{21}(\tau_B/N_{\rm H\,I})\ {\rm cm}^{-2}$, where τ_B is the extinction optical depth in the B band in the rest frame of an absorber and $N_{\rm H\,I}$ is the column density of neutral hydrogen. We assume for the moment that k is the same in all damped Lyα systems. The difference between the indices of the observed and emitted spectra of a background quasar is then

$$\Delta\alpha \equiv \alpha_o^d - \alpha_e^d = -k \sum_a \left(\frac{N_{\rm H\,Ia}}{10^{21}\ {\rm cm}^{-2}} \right) \frac{d\xi(\lambda_a)}{d \ln \lambda_a}, \qquad (1)$$

where $\xi(\lambda_a) \equiv A(\lambda_a)/A(4400\ \text{Å})$ is the ratio of the extinction at the absorption wavelength λ_a to that in the B band, and the sum is over all damped Lyα systems along the line of sight (usually only one). The derivatives $d\xi(\lambda_a)/d \ln \lambda_a$ must be evaluated over the range $1216 \le (1 + z_a)\lambda_a/(1 + z_e) \le 1549$ Å, corre-

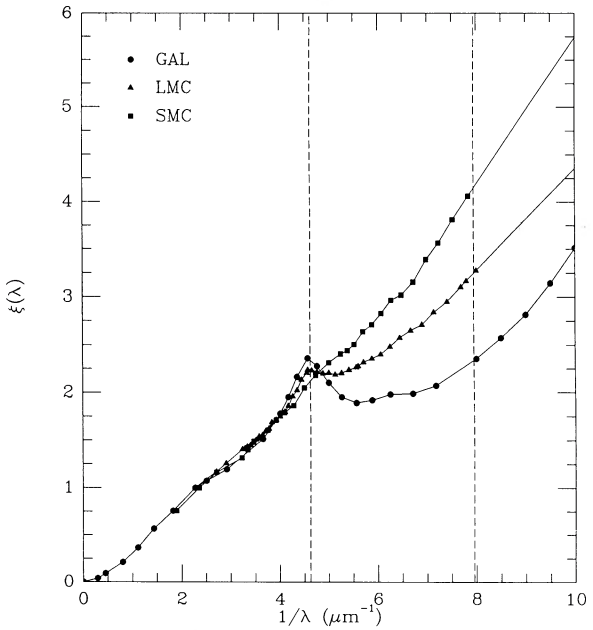

FIG. 3.—Normalized extinction curves for the Milky Way (Savage & Mathis 1979), LMC (Koornneef & Code 1981; Nandy et al. 1981), and SMC (Prévot et al. 1984). Extrapolations beyond the last measured points are of the form $\xi(\lambda) \propto \lambda^{-1}$. The vertical dashed lines bracket the range in which the derivatives $d\xi(\lambda)/d\ln\lambda$ were evaluated.

sponding to the range over which the spectral indices were determined. We perform all calculations with the "mean" extinction curves for the Milky Way and the Large and Small Magellanic Clouds (GAL, LMC, and SMC);[2] these are shown in Figure 3. The redshifts and H I column densities of the damped Lyα systems, mainly from Turnshek et al. (1989), are listed in Table 2.

Since the WTSC sample is unbiased with regard to absorption features and optical colors, we can assume that the indices of the emitted spectra in the damped and control subsamples, α_e^d and α_e^c, and therefore $\alpha_o^d - \Delta\alpha$ and α_o^c, were drawn at random from the same parent population. We derive the probability $P(<k)$ that the dust-to-gas ratio is less than k and the corresponding probability density $p(k) \equiv dP(<k)/dk$ using a Mann-Whitney U-test. Details of the method can be found in Papers I and II. Our results are shown in Figure 4 for the three different extinction curves. The most probable values k_p, at the peaks of $p(k)$, are listed in Table 3 along with positive and negative errors computed from the formulae

$$\sigma_+^2 = \int_{k_p}^{\infty} dk(k - k_p)^2 p(k) \Big/ \int_{k_p}^{\infty} dk p(k) , \qquad (2a)$$

$$\sigma_-^2 = \int_{0}^{k_p} dk(k - k_p)^2 p(k) \Big/ \int_{0}^{k_p} dk p(k) . \qquad (2b)$$

For comparison, the dust-to-gas ratio in the Milky Way is $k = 0.79$. We find that the most probable values of the dust-to-

[2] The LMC extinction curve adopted here actually pertains to the 30 Doradus region and might not be representative of the LMC as a whole (Clayton & Martin 1985; Fitzpatrick 1986). A similar caveat applies to the SMC extinction curve, which was derived from only a few stars. Nevertheless, the Galactic, LMC, and SMC extinction curves plotted in Figure 3 are suitable for our purposes because they span a wide range of possibilities and provide a sequence with decreasing strength of the bump at $\lambda_a \approx 2175$ Å.

TABLE 2

WTSC DAMPED SUBSAMPLE

Quasar	z_a	$N_{\rm H\,I}/10^{21}$ cm^{-2}	Reference
Q0100+130	2.31	2.5	1
Q0149+336	2.14	0.4	2
Q0458−020	2.04	5.0	2
Q1136+122	1.79	0.1	2
Q1151+068	1.77	1.8	2
Q1215+333	2.00	1.0	2
Q1244+347	1.86	0.4	2
Q1337+113	2.51	0.1	3
	2.80	0.8	2
Q1347+112	2.47	0.2	2
Q2136+141	2.14	0.2	2
Q2206−199N	1.92	0.7	4
	2.08	0.5	4
Q2348−011	2.43	0.3	2
	2.62	1.8	2
Q2359−022	2.10	0.5	2
	2.15	0.2	2

REFERENCES.—(1) Black, Chaffee, & Foltz 1987; (2) Turnshek et al. 1989; (3) Lanzetta, Wolfe, & Turnshek 1989; (4) Robertson, Shaver, & Carswell 1983.

TABLE 3

DUST-TO-GAS RATIOS AND OPTICAL DEPTHS

Sample	$\xi(\lambda)$	k_p	τ_{Bp}
WTSC	GAL	$0.36^{+0.36}_{-0.11}$	$0.40^{+0.22}_{-0.10}$
$\langle z_a\rangle = 2.18 \pm 0.07$	LMC	$0.09^{+0.15}_{-0.03}$	$0.12^{+0.06}_{-0.04}$
$\langle N_{\rm H\,I}\rangle = (1.0 \pm 0.3) \times 10^{21}$ cm^{-2}	SMC	$0.06^{+0.08}_{-0.02}$	$0.08^{+0.03}_{-0.02}$
SSB	GAL	$0.34^{+0.14}_{-0.11}$	$0.22^{+0.10}_{-0.07}$
$\langle z_a\rangle = 2.57 \pm 0.11$	LMC	$0.09^{+0.04}_{-0.03}$	$0.06^{+0.03}_{-0.02}$
$\langle N_{\rm H\,I}\rangle = (0.7 \pm 0.2) \times 10^{21}$ cm^{-2}	SMC	$0.06^{+0.02}_{-0.02}$	$0.04^{+0.02}_{-0.01}$
WTSC + SSB	GAL	$0.35^{+0.24}_{-0.09}$	$0.30^{+0.11}_{-0.06}$
$\langle z_a\rangle = 2.35 \pm 0.08$	LMC	$0.09^{+0.06}_{-0.02}$	$0.09^{+0.03}_{-0.02}$
$\langle N_{\rm H\,I}\rangle = (0.9 \pm 0.2) \times 10^{21}$ cm^{-2}	SMC	$0.06^{+0.03}_{-0.01}$	$0.06^{+0.02}_{-0.01}$

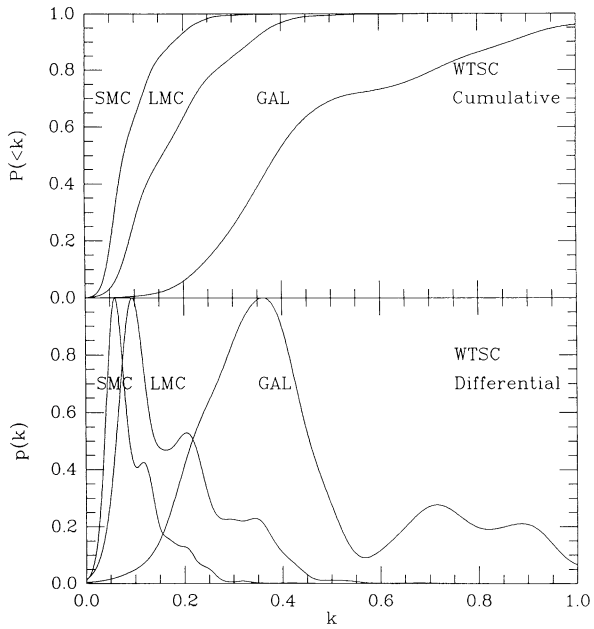

FIG. 4.—Cumulative and differential probabilities derived for the WTSC sample with the Galactic, LMC, and SMC extinction curves. The most probable values of the dust-to-gas ratio differ from zero at the 3 σ level.

gas ratio in the damped Lyα systems differ from zero at the 3 σ level and are 46% (GAL), 11% (LMC), and 8% (SMC) of that in the Milky Way.

Q2136+141, with $\alpha_o = 2.91$, is by far the reddest quasar in our sample. We are confident this is not an error because the spectra from different observing runs are in excellent agreement. If the index of the emitted spectrum of Q2136+141 were equal to the mean in the control subsample and the reddening were caused entirely by the foreground damped Lyα system, the dust-to-gas ratio and rest-frame optical depth would be $k \approx 3$–14 and $\tau_B \approx 0.5$–2.7. Another possibility is that some of the reddening is intrinsic to the quasar rather than the damped Lyα system. We also note that the correction for Galactic reddening toward Q2136+141 is the least certain in our sample and might have been underestimated. Because we use a nonparametric test to compare the spectral indices, our results are not sensitive to outlying points such as Q2136+141. In fact, if this quasar were eliminated from the sample, the significance of the reddening would remain above 99%, and the most probable values of the dust-to-gas ratio would decrease by only 4%.

4. DUST-TO-GAS RATIOS: THE SSB AND COMBINED SAMPLES

The detection of dust reported in Paper II was based on the eight strongest damped Lyα systems identified in the low-resolution SSB spectra. Since then, Lanzetta et al. (1991) have observed several of the weaker, candidate damped Lyα systems at intermediate resolution. The redshifts and H I column densities of the 13 confirmed damped Lyα systems in the SSB sample are listed in Table 4. According to Lanzetta et al., the identification of damped Lyα systems in both the WTSC and SSB samples is now complete or nearly so for $N_{\rm H\,I} \geq 2 \times 10^{20}$ cm^{-2}. We use the new identifications to improve our estimates of the dust-to-gas ratio in the SSB sample. The damped subsample consists of the nine quasars in Table 4 and the control subsample consists of 33 quasars without damped Lyα systems in the foreground. (We exclude from this analysis all spectra with broad absorption line (BAL) features or unconfirmed candidate damped Lyα features.) The reddening, shown in Figure 5, is significant at the 99.9% confidence level. In this case, the mean spectral indices in the two subsamples are $\langle \alpha_o^d \rangle = 0.90 \pm 0.07$ and $\langle \alpha_o^c \rangle = 0.66 \pm 0.04$. The results of the U-tests are shown in Figure 6, and the most probable values of the dust-to-gas ratio are listed in Table 3. These agree almost perfectly with our estimates from the WTSC sample. The dust-to-gas ratios derived in Paper II are 30%–40%, about 1 σ, lower than our new estimates.

We now combine the WTSC and SSB samples to make a more sensitive test for reddening in the damped Lyα systems. The justification for this is that the random errors in the two sets of spectral indices are similar, and any systematic differences between them are small. For the four quasars in

TABLE 4

SSB DAMPED SUBSAMPLE

Quasar	z_a	$N_{\rm H\,I}/10^{21}$ cm^{-2}	Reference
Q0000−263	3.39	2.0	1
Q0045−036	2.81	0.1	2
Q0102−190	2.37	1.0	1
Q0112+029	2.42	1.0	1
Q0201+365	2.46	0.3	2
Q0528−250	2.14	0.5	3
	2.81	1.3	4
Q2233+131	2.55	0.1	2
	3.15	0.1	2
Q2348−011	2.43	0.3	5
	2.62	1.8	5
Q2359−022	2.10	0.5	5
	2.15	0.2	5

REFERENCES.—(1) Sargent, Steidel, & Boksenberg 1989; (2) Lanzetta et al. 1991; (3) Morton et al. 1980; (4) Foltz, Chaffee, & Black 1988; (5) Turnshek et al. 1989.

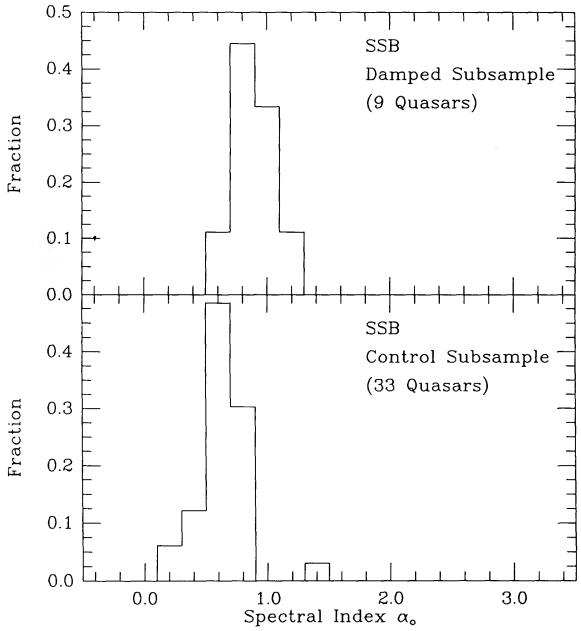

FIG. 5.—Histograms of the observed spectral indices in the SSB damped and control subsamples. The former are redder than the latter at the 99.9% confidence level.

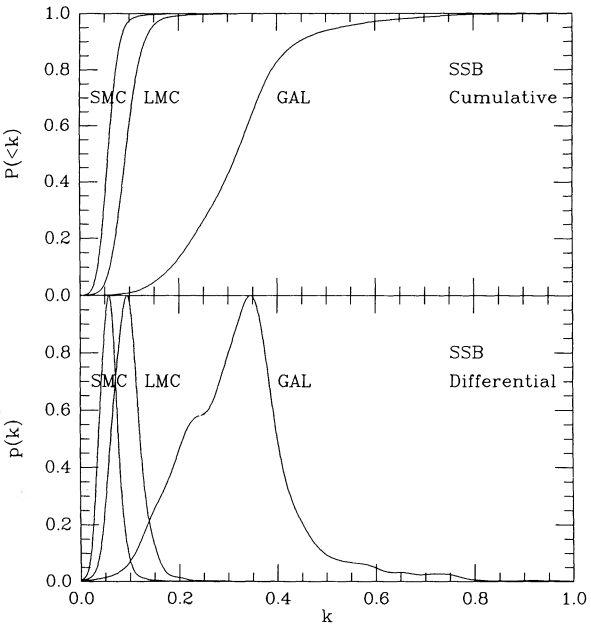

FIG. 6.—Cumulative and differential probabilities derived for the SSB sample with the Galactic, LMC, and SMC extinction curves. The most probable values of the dust-to-gas ratio differ from zero at the 3 σ level.

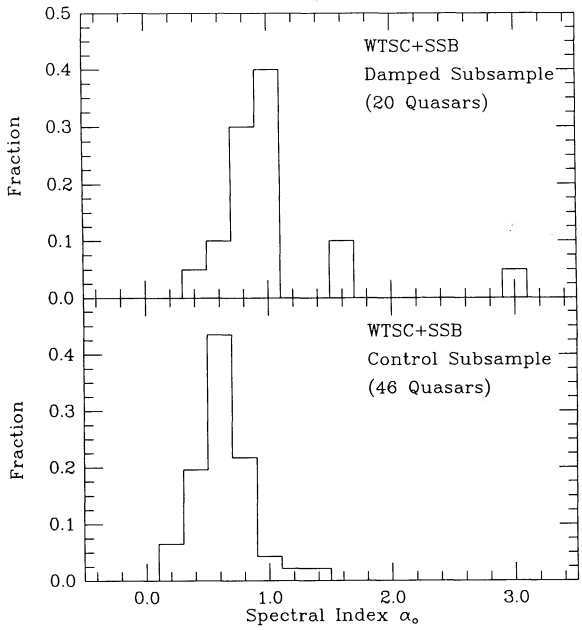

FIG. 7.—Histograms of the observed spectral indices in the combined WTSC and SSB damped and control subsamples. The former are redder than the latter at the 99.999% confidence level.

common, we average our values of α_o with the SSB values. The combined damped and control subsamples have, respectively, 20 and 46 quasars. The redshifts and column densities of the damped Lyα systems span the ranges $1.8 \leq z_a \leq 3.4$ and $1 \times 10^{20} \leq N_{\rm H\,I} \leq 5 \times 10^{21}$ cm^{-2}. Figure 7 shows histograms of the observed spectral indices in the two subsamples. In this case, the reddening is significant at the 99.999% level, and the mean spectral indices are $\langle \alpha_o^d \rangle = 1.02 \pm 0.12$ and $\langle \alpha_o^c \rangle = 0.64 \pm 0.04$. The cumulative and differential probabilities of the dust-to-gas ratio are shown in Figure 8 for the three different extinction curves. Our estimates of k_p, listed in Table 3, now differ from zero at or above the 4 σ level. They are 44% (GAL), 11% (LMC), and 8% (SMC) of the dust-to-gas ratio in the Milky Way. We obtain nearly identical results when all radio-loud quasars are excluded from the damped and control subsamples. Unfortunately, even the combined sample is not large enough to reveal a significant dependence of the dust-to-gas ratio on the redshifts or column densities of the damped Lyα systems.

We have made two checks that our results are not biased by the assumption of a constant dust-to-gas ratio. First, we repeated the analysis above assuming instead that all damped Lyα systems have the same rest-frame optical depth τ_B. In this case, equation (1) becomes $\Delta\alpha = -\tau_B \sum_a d\xi(\lambda_a)/d\ln\lambda_a$. The most probable values of the optical depth τ_{Bp} and the corresponding errors are listed in Table 3 for the WTSC, SSB, and combined samples. These are very close to the estimates we would have obtained from the naive relation $\tau_{Bp} \approx k_p \langle N_{\rm H\,I} \rangle / 10^{21}$ cm^{-2} with the dust-to-gas ratios derived previously and the mean column densities in the damped subsamples. Second, we performed a series of Monte Carlo simulations in which the individual dust-to-gas ratios were drawn at random from log-normal distributions with different dispersions $\sigma(\ln k)$ and means $\langle \ln k \rangle$. For $\sigma(\ln k) \lesssim 2$, the values of $\langle \ln k \rangle$ that are compatible with the observed spectral indices do not differ significantly from $\ln k_p$. We conclude that, although there may be large variations in the dust-to-gas ratio among individual damped Lyα systems, the most probable values given above can be considered typical of the population as a whole.

5. UPPER LIMITS ON GALACTIC-TYPE DUST

The different strengths of the bump at $\lambda_a \approx 2175$ Å in the assumed extinction curves of the damped Lyα systems account for most of the uncertainty in the dust-to-gas ratio derived from the reddening. This can be understood by referring to equation (1) and Figure 3. In the range of absorption wavelengths relevant to our analysis, $1260 \lesssim \lambda_a \lesssim 2160$ Å, the derivatives $|d\xi(\lambda_a)/d\ln\lambda_a|$ decrease as the strength of the bump increases, implying larger k for a given $\Delta\alpha$. However, the same bump in the Galactic extinction curve that gives rise to the largest estimates of the dust-to-gas ratio in the damped Lyα systems would also produce broad absorption features centered at $\lambda_a \approx 2175$ Å in the spectra of the background quasars. McKee & Petrosian (1974) pointed out that the absence of such features would constrain the abundance of Galactic-type dust along the lines of sight. The null results of subsequent searches for excess extinction at $\lambda_a \approx 2175$ Å in damped Lyα systems are summarized in Paper II. In three out of five cases, the upper limits on the dust-to-gas ratio are about 10% of the value in the Milky Way.

The spectra used in the search for Galactic-type dust should ideally cover the range of absorption wavelengths $1800 \lesssim \lambda_a \lesssim 2500$ Å (see Fig. 3). Our spectra do not satisfy this condition because they were obtained primarily to determine spectral indices at somewhat shorter wavelengths. Nevertheless, for the five damped Lyα systems with the lowest redshifts, the ends of our spectra at $\lambda_o = 6900$ Å correspond to $\lambda_a \approx 2300$–2500 Å, and a search for excess extinction is just possible. With this in mind, we have fitted the function

$$f_\lambda = f_e \lambda^{\alpha_e - 2} \exp\{-\tau_B \xi[\lambda/(1+z_a)]\} \quad (3)$$

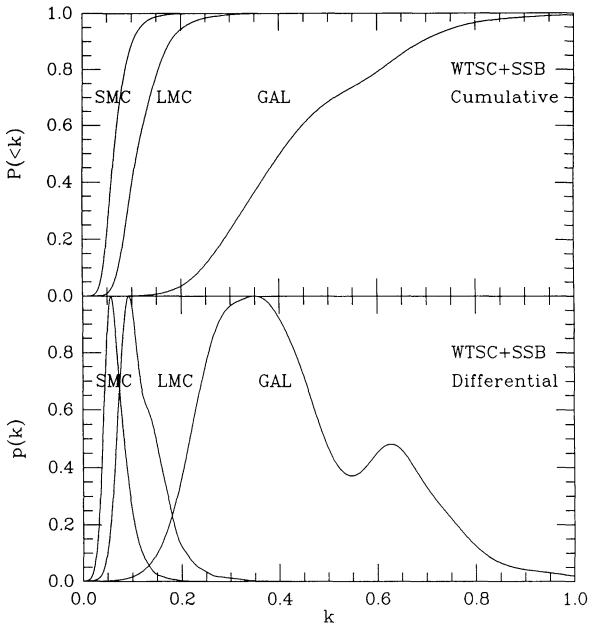

FIG. 8.—Cumulative and differential probabilities derived for the combined WTSC and SSB sample with the Galactic, LMC, and SMC extinction curves. The most probable values of the dust-to-gas ratio differ from zero at or above the 4 σ level.

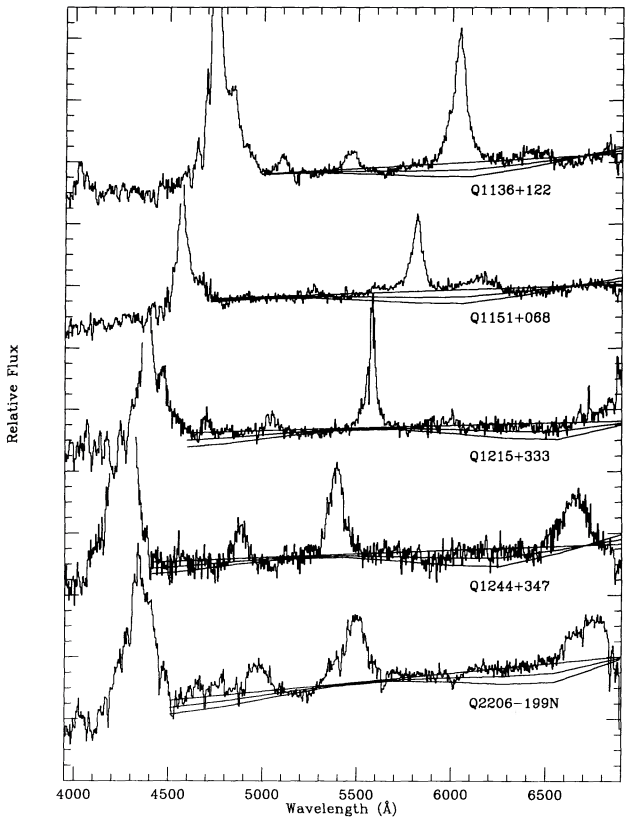

FIG. 9.—Spectra of quasars in the WTSC sample with damped Lyα systems at $z_a \leq 2.0$. The solid curves are least-square fits in the form of eq. (3) with the Galactic extinction curve and rest-frame optical depths $\tau_B = 0.0$, 0.3, and 0.6.

to the spectra shown in Figure 9. We determine the parameters f_e, α_e, and τ_B after the removal of emission and absorption lines by the procedure described in § 2. The solid curves in Figure 9 show the results of fixing the rest-frame optical depth at $\tau_B = 0.0$, 0.3, and 0.6 and minimizing χ^2 with respect to the amplitudes f_e and indices α_e of the emitted spectra. Evidently, the solutions with Galactic-type dust and $\tau_B \gtrsim 0.3$ do not provide acceptable fits to the observed spectra.

We give the 95% upper limits on the rest-frame optical depths of the five damped Lyα systems with the lowest redshifts in Table 5 for the Galactic, LMC, and SMC extinction curves. As expected, the values of τ_{B95} increase as the strength of the bump at $\lambda_a \approx 2175$ Å decreases. Our limits on the optical depths, when translated into limits on the dust-to-gas ratios, are similar to the constraints derived in previous searches (see Table 1 of Paper II). A comparison of Tables 3 and 5 shows that, for Galactic-type dust, the most probable values of

TABLE 5

UPPER LIMITS ON EXCESS EXTINCTION AT $\lambda_a \approx 2175$ Å

Quasar	τ_{B95} (GAL)	τ_{B95} (LMC)	τ_{B95} (SMC)
Q1136+122	0.01	0.02	0.14
Q1151+068	0.05	0.09	0.18
Q1215+333	0.10	0.12	0.18
Q1244+347	0.25	0.44	1.08
Q2206−199N	0.03[a]	0.07[a]	0.16[a]

[a] Based on the mean redshift of the damped Lyα systems with $z_a = 1.92$ and $z_a = 2.08$.

the optical depth τ_{Bp} derived from the spectral indices are not compatible with the upper limits τ_{B95} derived from the searches for excess extinction at $\lambda_a \approx 2175$ Å. However, for LMC-type dust, τ_{Bp} and τ_{B95} are marginally compatible, and for SMC-type dust, they are entirely compatible. The weak or absent bump in the extinction curve might indicate that the proportion of graphite relative to silicates is lower in the damped Lyα systems than in the Milky Way. In any case, the most probable values of the dust-to-gas ratio and the 1 σ errors derived with the LMC and SMC extinction curves lie in the range $0.05 \lesssim k \lesssim 0.15$, corresponding roughly to 5%–20% of the Galactic value. We adopt this range as our best estimate of the typical dust-to-gas ratio in the damped Lyα systems.

6. RELATIONS BETWEEN DUST AND HEAVY ELEMENTS

The abundances of heavy elements in the damped Lyα systems are likely to provide important clues about the chemical enrichment of galaxies at high redshifts. Unfortunately, the readily observable lines of the most common elements are highly saturated, and the abundances inferred from equivalent widths are uncertain by at least two orders of magnitude (Turnshek et al. 1989). One solution to this problem is to determine the degree of saturation from spectra of higher resolution (Rauch et al. 1990). Another approach is to observe the λλ2026, 2063 doublet of Zn II and the λλ2056, 2062, 2066 triplet of Cr II, both of which should be on or near the linear part of the curve of growth for modest values of the Doppler parameter ($b \gtrsim 3$ km s^{-1}). Results are now available for the three damped Lyα systems listed in Table 6 from Meyer, Welty, & York (1989), Meyer & Roth (1990), and Pettini, Boksenberg, & Hunstead (1990). These authors use the gas-phase abundance of Zn as an indicator of the overall level of chemical enrichment and the depletion of Cr relative to Zn as an indicator of the dust-to-gas ratio. A concern here is that inferences about the solid phase of the interstellar medium from gas-phase abundances alone are often sensitive to the assumed composition of the grains (Jenkins, Savage, & Spitzer 1986). We now consider the obser-

TABLE 6

ABUNDANCES OF HEAVY ELEMENTS

Quasar	z_a	δ(Zn)	δ(Cr)	Reference	Z/Z_G Eq. (7)	k/k_G Eq. (8)	Z/Z_G Eq. (9)	Z/Z_G Eq. (10)
Q0100+130	2.31	0.04	0.01	1, 2	0.03–0.13	0.02–0.12	0.03–0.17	0.06–0.21
Q0528−250	2.81	0.12	0.03	3	0.10–0.35	0.06–0.34	0.10–0.28	0.07–0.23
Q2206−199N	1.92	0.19	0.08	2	0.14–0.53	0.04–0.48	0.14–0.36	0.10–0.30

NOTES.—Entries in the last four columns are based on the assumption $\epsilon = \epsilon' = 0$ and include uncertainties of ±30% in δ(Zn), δ(Cr), $\delta(\mathrm{Zn})_G$, and $\delta(\mathrm{Cr})_G$. Those in the last two columns also include the range $0.05 \leq k/k_G \leq 0.20$ derived from the typical reddening.

REFERENCES.—(1) Pettini, Boksenberg, & Hunstead 1990; (2) Meyer & Roth 1990; (3) Meyer, Welty, & York 1989.

vations of Zn and Cr in the damped Lyα systems with this possibility in mind.

The total abundance of any element is the sum of the abundances in the gas and solid phases; hence

$$\mathrm{Zn^{tot}} = \mathrm{Zn^{gas}} + \mathrm{Zn^{sol}}\,, \quad \mathrm{Cr^{tot}} = \mathrm{Cr^{gas}} + \mathrm{Cr^{sol}}\,. \tag{4}$$

We relate these to the overall abundance of heavy elements Z and the dust-to-gas ratio k, in units of the Galactic values, Z_G and k_G, as follows:

$$\frac{(\mathrm{Zn^{tot}/H})}{(\mathrm{Zn^{tot}/H})_G} = (1 + \epsilon_{\mathrm{Zn}})\frac{Z}{Z_G}\,, \tag{5a}$$

$$\frac{(\mathrm{Cr^{tot}/H})}{(\mathrm{Cr^{tot}/H})_G} = (1 + \epsilon_{\mathrm{Cr}})\frac{Z}{Z_G}\,, \tag{5b}$$

$$\frac{(\mathrm{Zn^{sol}/H})}{(\mathrm{Zn^{sol}/H})_G} = (1 + \epsilon'_{\mathrm{Zn}})\frac{k}{k_G}\,, \tag{6a}$$

$$\frac{(\mathrm{Cr^{sol}/H})}{(\mathrm{Cr^{sol}/H})_G} = (1 + \epsilon'_{\mathrm{Cr}})\frac{k}{k_G}\,. \tag{6b}$$

The parameters ϵ and ϵ' allow for different patterns of nucleosynthesis and compositions of grains in the damped Lyα systems. The only constraints on ϵ and ϵ' are that they lead to nonnegative values of Z/Z_G and k/k_G. Setting $(\mathrm{Zn^{tot}/H})_G \approx (\mathrm{Zn/H})_\odot$ and $(\mathrm{Cr^{tot}/H})_G \approx (\mathrm{Cr/H})_\odot$ and solving equations (4)–(6), we obtain

$$\frac{Z}{Z_G} \approx \frac{(1 + \epsilon'_{\mathrm{Cr}})\delta(\mathrm{Zn})[1 - \delta(\mathrm{Cr})_G] - (1 + \epsilon'_{\mathrm{Zn}})\delta(\mathrm{Cr})[1 - \delta(\mathrm{Zn})_G]}{(1 + \epsilon'_{\mathrm{Cr}})(1 + \epsilon_{\mathrm{Zn}})[1 - \delta(\mathrm{Cr})_G] - (1 + \epsilon'_{\mathrm{Zn}})(1 + \epsilon_{\mathrm{Cr}})[1 - \delta(\mathrm{Zn})_G]}\,, \tag{7}$$

$$\frac{k}{k_G} \approx \frac{(1 + \epsilon_{\mathrm{Cr}})\delta(\mathrm{Zn}) - (1 + \epsilon_{\mathrm{Zn}})\delta(\mathrm{Cr})}{(1 + \epsilon'_{\mathrm{Cr}})(1 + \epsilon_{\mathrm{Zn}})[1 - \delta(\mathrm{Cr})_G] - (1 + \epsilon'_{\mathrm{Zn}})(1 + \epsilon_{\mathrm{Cr}})[1 - \delta(\mathrm{Zn})_G]}\,, \tag{8}$$

where the deltas denote gas-phase abundances in units of the Solar values, e.g., $\delta(\mathrm{Zn}) \equiv (\mathrm{Zn^{gas}/H})/(\mathrm{Zn/H})_\odot$.

We have computed the overall abundances of heavy elements and the dust-to-gas ratios in the damped Lyα systems from equations (7) and (8) with the published gas-phase abundances of Zn and Cr. For the Galactic depletions, we adopt the standard values $\delta(\mathrm{Zn})_G = 0.6$ and $\delta(\mathrm{Cr})_G = 0.02$ (York & Jura 1982; de Boer et al. 1986; Harris & Mas Hesse 1986; Van Steenberg & Shull 1988). Our estimates of Z/Z_G and k/k_G for $\epsilon = \epsilon' = 0$ are listed in the sixth and seventh columns of Table 6. The ranges given there reflect plausible uncertainties of $\pm 30\%$ in $\delta(\mathrm{Zn})$, $\delta(\mathrm{Cr})$, $\delta(\mathrm{Zn})_G$, and $\delta(\mathrm{Cr})_G$. Typical values of Z/Z_G and k/k_G are of order 0.1, consistent with the estimates by Meyer et al. (1989), Meyer & Roth (1990), and Pettini et al. (1990).[3] However, if we no longer assume that the abundance ratios and grain compositions in the damped Lyα systems are the same as those in the Milky Way, the denominators of equations (7) and (8) can become very small and the estimates of Z/Z_G and k/k_G very large. This occurs, for example, for $\epsilon_{\mathrm{Zn}} \approx \epsilon'_{\mathrm{Cr}} \approx -0.2$ and $\epsilon_{\mathrm{Cr}} \approx \epsilon'_{\mathrm{Zn}} \approx +0.2$. Unless such values can somehow be ruled out, the gas-phase abundances of Zn and Cr by themselves can only be used to set lower limits on the overall abundances of heavy elements in the damped Lyα systems. They do not constrain the dust-to-gas ratios and therefore do not establish upper limits on the overall abundances.

We can eliminate some of this ambiguity by combining the measurements of Zn and Cr with the typical dust-to-gas ratio derived from the reddening of background quasars. Equations (4)–(6) have the alternative solutions

$$\frac{Z}{Z_G} \approx \frac{1}{(1 + \epsilon_{\mathrm{Zn}})}\left\{\delta(\mathrm{Zn}) + \frac{k}{k_G}(1 + \epsilon'_{\mathrm{Zn}})[1 - \delta(\mathrm{Zn})_G]\right\}, \tag{9}$$

$$\frac{Z}{Z_G} \approx \frac{1}{(1 + \epsilon_{\mathrm{Cr}})}\left\{\delta(\mathrm{Cr}) + \frac{k}{k_G}(1 + \epsilon'_{\mathrm{Cr}})[1 - \delta(\mathrm{Cr})_G]\right\}. \tag{10}$$

These are much less sensitive than equations (7) and (8) to the assumed abundance ratios and grain compositions in the damped Lyα systems. For $0.05 \leq k/k_G \leq 0.20$, we obtain the results listed in the last two columns of Table 6. Our estimates of the overall abundances from k/k_G and $\delta(\mathrm{Zn})$ agree remarkably well with those from k/k_G and $\delta(\mathrm{Cr})$. They are also consistent with the estimates derived previously from the gas-phase abundances alone and the assumption $\epsilon = \epsilon' = 0$. Given the allowed ranges in Z/Z_G, there may or may not be real variations from one damped Lyα system to another. We can, however, conclude that, if this small sample is representative of the population as a whole, the overall abundances of heavy elements in the damped Lyα systems at $2 \lesssim z \lesssim 3$ are about one order of magnitude lower than that in the Milky Way today.

We are grateful to L. Cowie, R. W. Hunstead, and L. Spitzer for helpful discussions. J. B. acknowledges support from the National Science Foundation through grants RII 8800660 and AST 9058510.

[3] For $\delta(\mathrm{Zn})_G = 1$, $\delta(\mathrm{Cr})_G \ll 1$, and $\epsilon = \epsilon' = 0$, eqs. (7) and (8) reduce to $Z/Z_G \approx \delta(\mathrm{Zn})$ and $k/k_G \approx \delta(\mathrm{Zn}) - \delta(\mathrm{Cr})$. These expressions give the values of Z/Z_G and k/k_G quoted by Meyer & Roth (1990).

REFERENCES

Black, J. H., Chaffee, F. H., & Foltz, C. B. 1987, ApJ, 317, 442
Burstein, D., & Heiles, C. 1982, AJ, 87, 1165
Clayton, G. C., & Martin, P. G. 1985, ApJ, 288, 558
de Boer, K. S., Lenhart, H., van der Hucht, K. A., Kamperman, T. M., Kondo, Y., & Bruhweiler, F. C. 1986, A&A, 157, 119
Fall, S. M., & Pei, Y. C. 1989, ApJ, 337, 7 (Paper I)
Fall, S. M., Pei, Y. C., & McMahon, R. G. 1989, ApJ, 341, L5 (Paper II)
Fitzpatrick, E. L. 1986, AJ, 92, 1068
Foltz, C. B., Chaffee, F. H., & Black, J. H. 1988, ApJ, 324, 267
Harris, A. W., & Mas Hesse, J. M. 1986, MNRAS, 220, 271
Hewitt, A., & Burbidge, G. 1987, ApJS, 63, 1
Jenkins, E. B., Savage, B. D., & Spitzer, L. 1986, ApJ, 301, 355
Koornneef, J., & Code, A. D. 1981, ApJ, 247, 860
Lanzetta, K. M., Wolfe, A. M., & Turnshek, D. A. 1989, ApJ, 344, 277
Lanzetta, K. M., Wolfe, A. M., Turnshek, D. A., Lu, L. M., McMahon, R. G., & Hazard, C. 1991, ApJS, in press
McKee, C. F., & Petrosian, V. 1974, ApJ, 189, 17
Meyer, D. M., & Roth, K. C. 1990, ApJ, 363, 57
Meyer, D. M., Welty, D. E., & York, D. G. 1989, ApJ, 343, L37
Morton, D. C., Chen, J. S., Wright, A. E., Peterson, B. A., & Jauncey, D. L. 1980, MNRAS, 193, 399
Nandy, K., Morgan, D. H., Willis, A. J., Wilson, R., & Gondhalekar, P. M. 1981, MNRAS, 196, 955
Pettini, M., Boksenberg, A., & Hunstead, R. W. 1990, ApJ, 348, 48

Prévot, M. L., Lequeux, J., Maurice, E., Prévot, L., & Rocca-Volmerange, B. 1984, A&A, 132, 389
Rauch, M., Carswell, R. F., Robertson, J. G., Shaver, P. A., & Webb, J. K. 1990, MNRAS, 242, 698
Robertson, J. G., Shaver, P. A., & Carswell, R. F. 1983, in Quasars and Gravitational Lenses, ed. J. P. Swings (Liège: University of Liège), 602
Sargent, W. L. W., Steidel, C. C., & Boksenberg, A. 1989, ApJS, 69, 703 (SSB)
Savage, B. D., & Mathis, J. S. 1979, ARA&A, 17, 73
Turnshek, D. A., Wolfe, A. M., Lanzetta, K. M., Briggs, F. H., Cohen, R. D., Foltz, C. B., Smith, H. E., & Wilkes, B. J. 1989, ApJ, 344, 567
Tyson, N. D. 1988, ApJ, 329, L57
Van Steenberg, M. E., & Shull, J. M. 1988, ApJ, 330, 942
Wolfe, A. M. 1988, in QSO Absorption Lines: Probing the Universe, ed. J. C. Blades, D. A. Turnshek, & C. A. Norman (Cambridge: Cambridge University Press), 297
———. 1990, in The Interstellar Medium in Galaxies, ed. H. A. Thronson & J. M. Shull (Dordrecht: Kluwer), 387
Wolfe, A. M., Turnshek, D. A., Smith, H. E., & Cohen, R. D. 1986, ApJS, 61, 249 (WTSC)
York, D. G., & Jura, M. 1982, ApJ, 254, 88